Influence of Amphiphilic Polymers on Corneal Wound Healing

Honors Research Thesis

Presented in Partial Fulfillment of the Requirements for the Degree Bachelor of Science with Honors Research Distinction in the Undergraduate School of The Ohio State University

By

Sophie Ann Carus

Undergraduate Biomedical Engineering

The Ohio State University

2018

Undergraduate Thesis Committee

Katelyn Swindle-Reilly, Ph.D., Advisor

Jennifer Leight, Ph.D.

Abstract

The cornea is the outermost layer of the eye, which makes it more susceptible to injury. In 2015 approximately 604,000 individuals in the US underwent some form of refractive laser surgery and many of those individuals developed corneal flaps created by the surgery that do not fully heal and do not completely reattach to the cornea even years after surgery (Riau et al., 2011). Additionally, 27% of all patient visits for ocular injuries are the result of corneal abrasions and lacerations (Ashby, Garrett, & Wilcox, 2014). Instances of improper corneal wound healing indicate a clinical need for a therapeutic method to improve corneal wound healing without scarring. Throughout the phases of corneal wound healing, fibroblasts and myofibroblasts proliferate and begin to form an extracellular matrix. When these fibroblasts and myofibroblasts are over expressed abnormal healing occurs resulting in opacity that frequently leads to the requirement of a corneal transplant. Many researchers have studied the mechanical and biological properties of healthy corneas while others have observed epithelial cell migration on therapeutic contact lenses after surgery. However, despite this extensive research there is a scientific gap in the understanding of how the chemical and mechanical properties of materials influence corneal wound healing. The purpose of this study aimed to identify the optimal surface free energy that promotes preferential attachment of corneal epithelial cells to ultimately design better materials, such as therapeutic bandage lenses, for use in corneal repair. Amphiphilic polymers with different ratios of 2-hydroxyethyl methacrylate (HEMA) and 3-methacryloxypropyl tris(trimethylsiloxy)silane (TRIS) were synthesized via free radical copolymerization to produce amphiphilic copolymers. Surface free energies were determined utilizing a goniometer to take contact angle measurements. Surface chemistry was further analyzed using FTIR. Seeding of NIH 3T3 fibroblast cells onto the polymer films was done to

determine cell attachment and viability differences between the polymers. Initial results indicate highest cellular viability on pure TRIS polymer with varying results for amphiphilic polymers. FTIR results indicated successful polymerization. Surface free energy testing produced inconclusive results with further testing needed to optimize film casting and goniometer methodology. Further experiments must be run to conclusively determine surface free energy of the amphiphilic polymers along with cell viability on the various polymers.

Acknowledgements

I would like to thank Dr. Swindle-Reilly for continuing to mentor me throughout this project. She has always been available to answer all of my questions regarding my research as well as other aspects of life in college. She always pushes me to work harder to improve myself as much as I can. I would also like to thank Dr. Ruegsegger for helping me with FTIR analysis and being willing to sit down and help me learn how to read the results I obtained. Additionally, I would like to thank my lab mates, Mallory Allen, Ryan Prieto, and Katrina Schroeder for their constant support and willingness to help with my experiments. I would also like to thank my family for being so supportive throughout college and for helping to push me to become the best I can be.

Vita

2014……..…St. Bede Academy High School, Peru, IL

2018…….……B.S. Biomedical Engineering, The Ohio State University

Fields of Study

Major Field: Biomedical Engineering

Table of Contents

List of Tables

List of Figures

Introduction:

The cornea forms the central external surface of the eye and constantly sheds epithelial layers, similar to the skin. These epithelial cells are shed into the tear pool and replaced by cells from the limbus moving centrally and from the basal layer anteriorly (Dua, Gomes, & Singh, 1994). The tear film provides the corneal epithelium with most of its oxygen supply while the aqueous humor supplies the bulk of the nutrients (Dua et al., 1994). There are many layers that make up the cornea starting with the epithelium on the exterior and ending with the endothelium on the interior (Figure 1). In addition to constant healing the cornea is also a transparent structure that helps to protect the rest of the eye and makes up two-thirds the refractive power of the eye (Chawla & Singh, 2017).

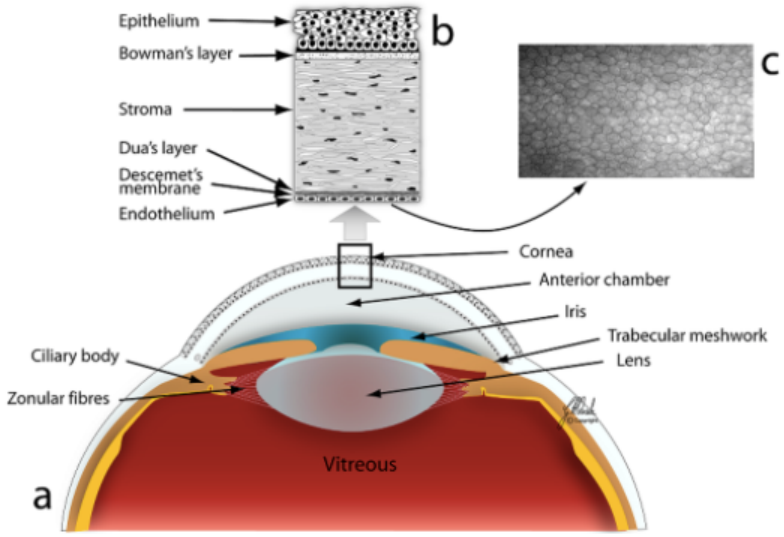

Figure 1: Diagram showing the anatomy of the cornea (Navaratnam et al., 2015).

Corneal epithelial wound healing is a complicated process that occurs after an injury to the epithelium of the cornea from a surgical wound, traumatic injury, chemical burn, or ultraviolet radiation exposure (Maycock & Marshall, 2014). Generally, the process can be categorized into three main phases: epithelial cell migration, proliferation, and adhesion (Dua et al., 1994). Epithelial cell migration consists of a latent phase and a linear healing phase. The

latent phase occurs 4-6 hours after the injury to the corneal epithelium when there is no visible healing taking place, but instead the epithelium surrounding the wound progressively thins and concentrations of fibronectin, fibrinogen, and fibrin increase on the surface of the wound (Dua et al., 1994). Cell-to-cell and cell-to-basement membrane attachments are also broken during the early phases of epithelial wound healing to allow for migration across the wounded area (Maycock & Marshall, 2014). During the linear phase the epithelial cells continue to flatten and begin to spread across the wound in a centripetal manner until the wound is completely covered (Dua et al., 1994).

The cell proliferation phase of corneal epithelial wound healing begins next and involves the restoration of cell numbers and cell mass to normal levels. This is done by a wave of mitosis from the edges of the wound towards the center. The basal epithelial cells are the main participants in this process of proliferation (Figure 2) (Dua et al., 1994). At this point fibroblasts and myofibroblasts become activated to help rebuild the extracellular matrix, sometimes forming scarred regions of corneal haze when overexpressed (Maycock & Marshall, 2014). Once proliferation and migration have occurred, the third phase begins with epithelial cell adhesions anchoring the cells to the underlying connective tissue, followed by hemidesmosomal attachments forming to firmly anchor the cells to the basement membrane (Dua et al., 1994) (Figure 2). The wing cell intracellular junctions provide the main structural integrity of the corneal epithelium and produce protein precursors that are needed for squamous cells to form tight junctions (Figure 2) (Ashby et al., 2014).

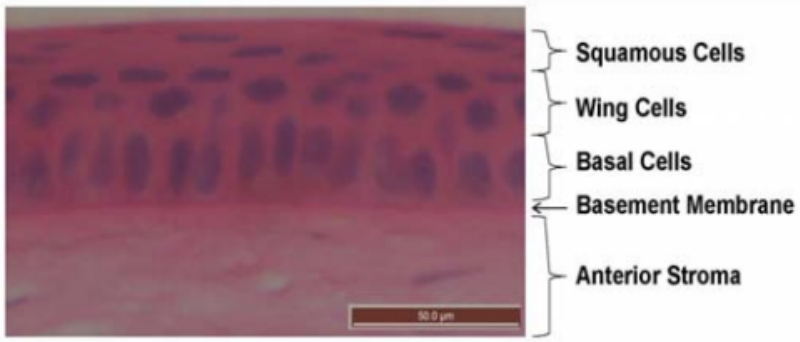

Figure 2: Image showing corneal epithelium layers via light micrograph at 60x (Ashby et al., 2014).

The cornea, being the outermost layer of the eye, is more susceptible to injury (Ashby et al., 2014). Specifically, corneal flaps created by refractive laser surgery (e.g. LASIK) do not fully heal and do not completely reattach to the cornea even years after surgery (Dupps & Wilson, 2006; Riau et al., 2011). Additionally, a study was performed to determine if corneal epithelial cells could be cultured onto therapeutic contact lenses after observing epithelial cell growth on lenses of patients who had undergone surgery (Di Girolamo, Chui, Wakefield, & Coroneo, 2006). This study provided evidence that polymers could play a vital role in enhancing corneal epithelial wound healing.

The in depth genomic and biological factors responsible for corneal epithelial wound healing have been extensively researched by several groups, while the biomechanical properties of native corneas have been studied by a variety of other researchers. However, there remains a scientific gap in the understanding of how the chemical and mechanical properties of materials influence corneal wound healing. This study aimed to identify the optimal surface energy (hydrophilicity/hydrophobicity) to promote preferential attachment of corneal epithelial cells to ultimately design better biomaterials, such as therapeutic bandage lenses, for use in corneal repair. This initial study looked into the effect certain amphiphilic polymers had on fibroblast cells, a main component present in the corneal epithelial wound healing process.

Materials and Methods:

Polymer Synthesis:

The optimal balance of hydrophobicity and hydrophilicity (surface free energy) was determined by synthesizing a variety of combinations of 3-methacryloxypropyl tris(trimethylsiloxy)silane (TRIS, hydrophobic silicone) and 2-hydroxyethyl methacrylate (HEMA, hydrophilic) polymers to develop of range of amphiphilic copolymers (Table 1) (Figure 3). TRIS and HEMA were used due to their well-known biocompatibility, use in contact lenses and intraocular lenses, and proven corneal epithelial cell growth in research (Di Girolamo, Chui, Wakefield, & Coroneo, 2006). These polymers were synthesized via free radical co-polymerization. Based on the molar ratios in Table 1, TRIS and HEMA monomers were weighed out into vials for a total weight of two grams. Seven grams of solvent was then added to each vial using isopropyl alcohol (IPA) for all polymers except pure TRIS which used isooctane. Isooctane is used commercially in wound care products and is therefore safe for use as a solvent. The initiator solution, 1.5% wt/wt 2,2'azobis-(2-methylbutyronitrile) (Vazo 67), was then prepared by mixing Vazo 67 with IPA and isooctane in separate flasks. One gram of initiator solution was needed to synthesize each polymer for a 1:2 initiator to monomer ratio and 20% wt/wt total monomer in solution. Polymerization was initiated by adding one gram of the corresponding Vazo 67 solution to each prepared polymer vial, bubbling N_2 gas into the solution for two minutes to purge the system of oxygen, and then placing the vial in a 70°C oil bath for six hours. Each vial was periodically swirled every thirty minutes.

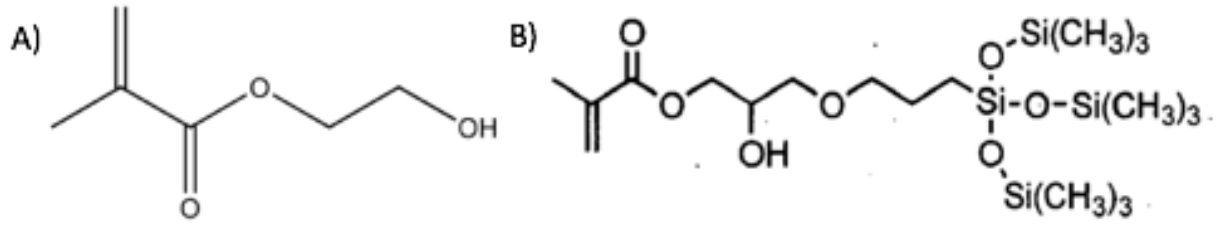

Figure 3: Image showing HEMA (A) and TRIS (B) monomers.

Following polymerization, the polymers were precipitated by adding the solutions dropwise to a 10-fold excess mixture of distilled water (DIH_2O) and methanol (MeOH) (Table 1) under high stirring conditions. Washes of distilled water and methanol were changed twice a day for five days, keeping the containers on a shaker to enhance removal of remaining monomers and impurities. On the fifth day, the washes were removed and the polymers were allowed to air dry for 24 hours. After 24 hours, the polymers were heated at a range between 70-80°C to remove any residual solvent. Polymers were then dissolved in a solvent at a 7% wt/wt ratio for use in casting films (Table 1).

Table 1: Breakdown of ratios and solvents used for polymer synthesis

Polymer Molar Ratio	Solvent for Polymerization and Vazo 67 Solution	Wash Volume Ratio		Solvent for Film Casting
		DIH_2O	MeOH	
TRIS	Isooctane	0%	100%	Isooctane
3:1 T:H	IPA	25%	75%	Isooctane
2:1 T:H	IPA	50%	50%	Isooctane
1:1 T:H	IPA	50%	50%	Isooctane
1:2 T:H	IPA	50%	50%	IPA
1:3 T:H	IPA	75%	25%	IPA
HEMA	IPA	100%	0%	IPA

Surface Free Energy and FTIR Testing:

Polymer films were made on standard 25 x 25 mm glass cover slips. 50 µL of each dissolved polymer was pipetted onto a glass cover slip. Once the solvent evaporated, 1 µL of DIH_2O and then mineral oil was placed on each polymer for contact angle measurements

utilizing a ramé-hart goniometer. This data was then analyzed within the DROPimage Advanced software to obtain total surface free energy for each polymer and contact angles for water and oil.

Another set of polymer films were made onto glass cover slips following the same protocol in the previous paragraph. Surface chemical analysis of the TRIS, HEMA and mixed films was then performed using a Thermo Nicolet Nexus670 FTIR spectrometer (Thermo Scientific, Waltham, MA) in the attenuated total reflectance (ATR) mode. A germanium crystal was placed in contact with each film sample and 100 scans were collected at an 8 cm^{-1} resolution. Peak analysis included determination of peak height for ester (1750 cm^{-1}), silicon-oxygen bonds (1055 cm^{-1}), methyl (3000 cm^{-1}), and alcohol (3200-3550 cm^{-1}) peaks without normalization or baseline correction.

Cell Culture:

NIH 3T3 fibroblast cells (ATCC CRL-1658) were cultured in T-75 culture flasks using Dulbecco's modified Eagle medium with 10% iron-fortified bovine calf serum (DMEM + 10% BCS). Mouse fibroblast cells were used for this preliminary study because they are more durable and still exhibit a fibroblast phenotype similar to fibroblasts involved in the corneal wound healing process. NIH 3T3 cells are also commonly used as a "feeder" cell layer for corneal epithelial cells (De Paiva, Pflugfelder, & Li, 2006). Cells were grown and passaged using 0.25% trypsin in ethylenediamine- tetraacetic acid (EDTA) along with standard cell culture techniques to acquire enough cells for the experiment. All of the cells were grown in a standard incubator at 37°C and 5% CO_2. A standard reusable hemocytometer was used to determine cell density.

Cell Viability Quantification:

Polymer films were created within sterile 12-well tissue culture plates. 100 μL of each dissolved polymer solution was pipetted into separate wells. One well was left empty as a control to form a total of 8 test samples. The solvent was allowed to evaporate for 48 hours and put under UV light for 2 hours to ensure sterility prior to cell seeding. Following recommended cell seeding densities for NIH 3T3 cells from the ATCC, 15,200 cells were seeded into each well. 1 mL of DMEM + 10% BCS was then added to each well and the media was only replaced on the third day. On days 1, 3, and 5 images were taken of each well using a light microscope at 10x magnification.

On the fifth day, an MTS (3-(4,5-dimethylthiazol-2-yl)-5-(3-carboxymethoxyphenyl)-2-(4-sulfophenyl)-2H-tetrazolium) assay was used to determine cell viability. An MTS assay is a colorimetric assay that determines how many metabolically active cells are in the culture based on the reduction of MTS tetrazolium dye by viable cells. 100 μL of MTS reagent was added to each well. Each well-plate was then placed in the incubator for 2 hours. After 2 hours, 220 μL of solution from each well was transferred to a 96-well plate. Three measurements were taken from each well for a total of 24 wells in the 96-well plate. Absorbances were measured at 490 nm using a SpectraMax M5 plate reader. The data was then plotted to determine cell viability under each polymer condition by first taking the average of the three absorbance readings for each well. The average absorbance from each polymer condition was then divided by the average absorbance from the control well and multiplied by 100. The graph was then created by plotting the viability percentages in a bar graph.

Results & Discussion:

Surface Free Energy and FTIR Testing:

Goniometer testing to determine the surface free energies of the seven polymers synthesized produced varied results. Generally, the surface free energy increased as the polymers acquired more HEMA with the exceptions of the TRIS:HEMA 2:1 and the TRIS:HEMA 1:1 polymer (Table 2). The water contact angle was larger with TRIS than with HEMA which is not expected when considering TRIS is more hydrophobic than HEMA. It is important to keep in mind that contact angle and surface energy are only characterizing the chemical orientation on the surface. Therefore, it is possible that since air is hydrophobic the hydrophilic groups on HEMA rotated in upon formation of a film due to their small size, resulting in an altered water contact angle and overall surface free energy.

The HEMA polymer films also exhibited irregular formation on the glass slides. They were more textured than the polymer films with TRIS. A rough surface topography could have also produced the unusual results obtained. However, SEM images would need to be acquired to prove this. The exact thickness of films was also unknown and in some cases the silicon from the glass slides may also have impacted the results obtained. Moving forward we will look into improved methods for film casting such as different solvents or materials to form the films. Additionally, there are alternative methods for obtaining contact angles and surface free energies such as receding or advancing contact angle measurements. These two methods involve taking multiple measurements while adding and removing drops of water or other liquid from a droplet on the surface of the material. These methods help to eliminate error that may have occurred due to surface chemistry at the start of the testing.

Table 2: Goniometer testing results showing water and oil contact angles and surface free energy for each polymer.

Polymer	Water Contact Angle	Oil Contact Angle	Surface Free Energy
TRIS	93.62 ± 0.06	62.29 ± 0.01	20.8 ± 0.02
T:H 3:1	89.6 ± 0.07	60.7 ± 0.01	22.78 ± 0.03
T:H 2:1	57.75 ± 0.09	23.05 ± 0.04	46.91 ± 0.06
T:H 1:1	90.17 ± 0.08	52.65 ± 0.01	24.31 ± 0.03
T:H 1:2	93.55 ± 0.06	51.37 ± 0.01	23.39 ± 0.02
T:H 1:3	89.28 ± 0.07	49.84 ± 0.04	25.3 ± 0.03
HEMA	90.6 ± 0.10	48.44 ± 0.02	25.11 ± 0.04

Due to the inconsistencies in the contact angle and surface free energy data further surface analysis of the polymers were performed through FTIR. The results from FTIR showed expression of the alcohol groups from HEMA present along with the ester groups from each polymer. The TRIS results clearly showed a strong peak at 1055 cm^{-1}, indicating the presence of the silicon-oxygen bonds seen in TRIS (Figure 4). There is a small peak within the TRIS data at 1726 cm^{-1} that most likely represents the presence of ester bonds. While a carbonyl stretch usually produces a large peak it is possible that the overpowering silicon-oxygen bonds present in TRIS may have outweighed the ester signals. FTIR calculates ratios of wavelengths. Therefore, with all of the silicon-oxygen bonds present in TRIS the ester peak may have been suppressed.

The results for the HEMA polymer clearly demonstrated a broad peak at 3400 cm^{-1}, representing the alcohol groups present on HEMA (Figure 4). These results also demonstrated a strong peak at 1720 cm^{-1} for the ester bonds as expected. Both the HEMA and TRIS results showed peaks around 3000 cm^{-1}, confirming the presence of methyl groups and in general all the carbon-hydrogen bonds present in both polymers. All FTIR results collected exhibited large peaks below 800 cm^{-1}. These unusual peaks may represent the FTIR picking up the surface chemistry of the glass slide below the polymer films since the polymer film thicknesses were

unknown. Further studies would have to be conducted to confirm this hypothesis, potentially by using the standard FTIR testing with KBr pellet.

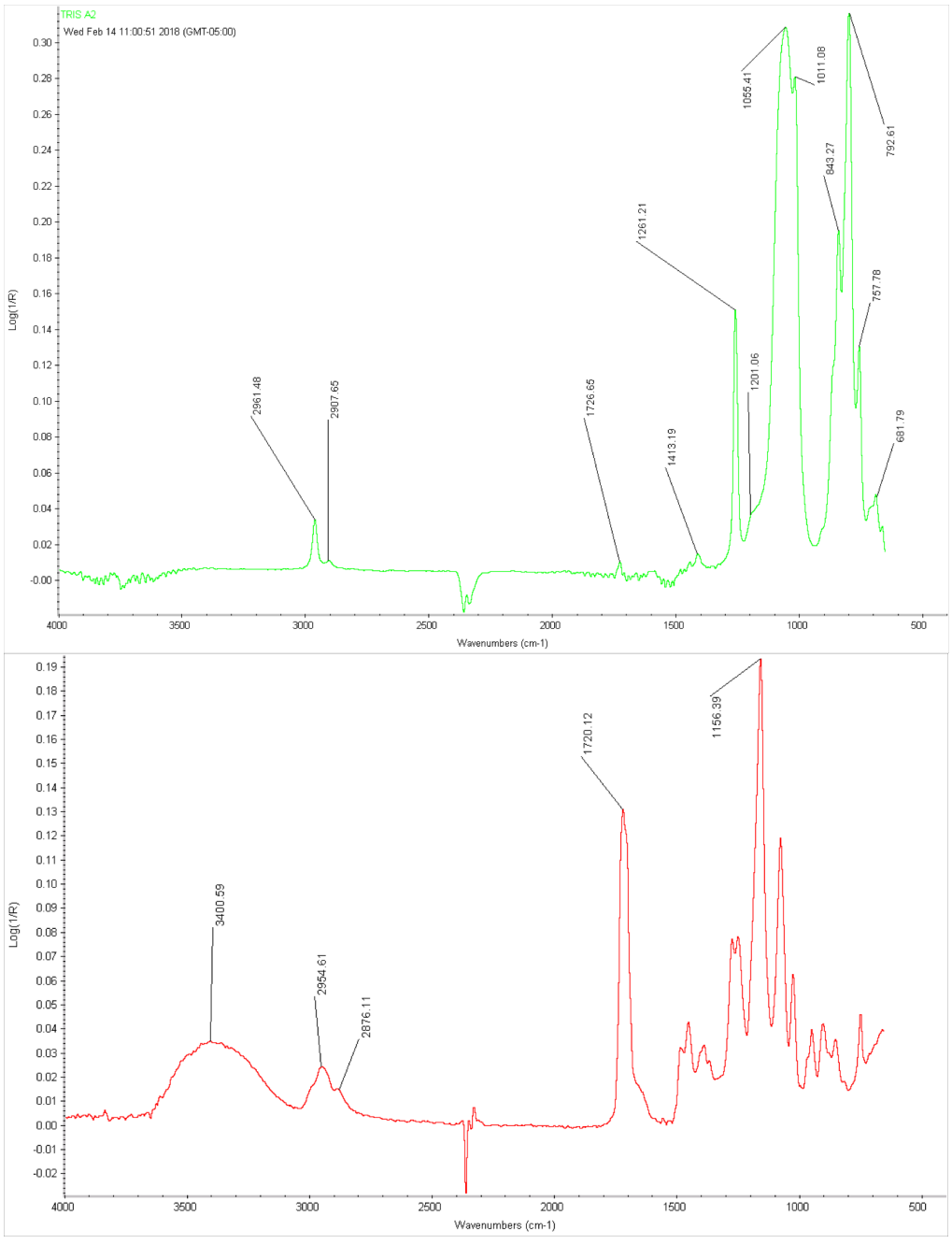

Figure 4: FTIR results from TRIS (top) and HEMA (bottom) polymers.

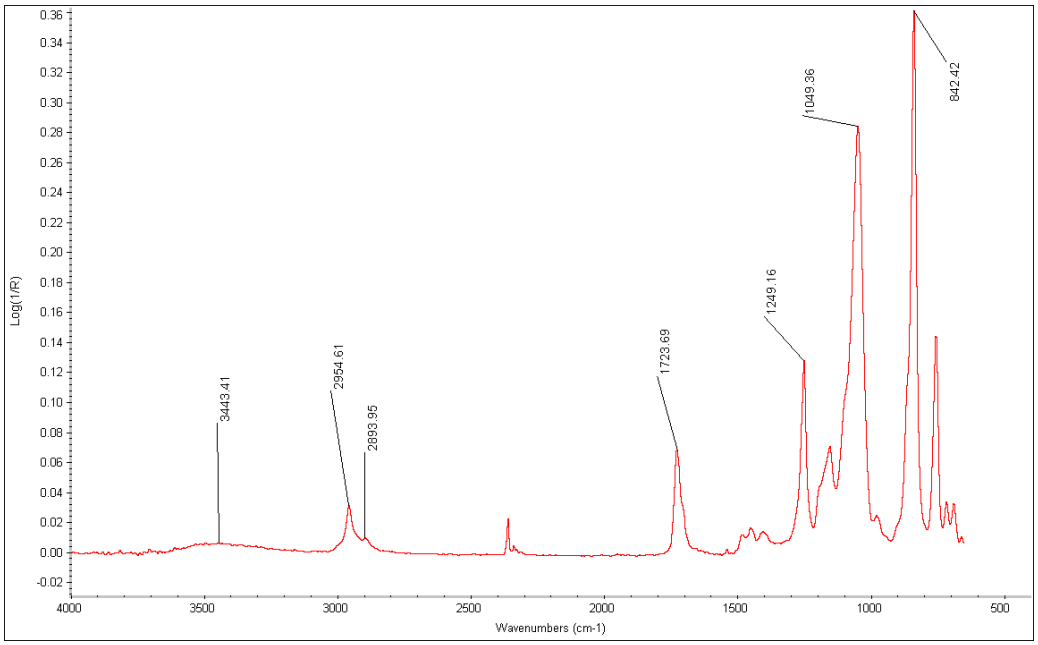

Figure 5: FTIR results for TRIS:HEMA 1:1 polymer.

FTIR results were also obtained for the various polymer ratios. In particular the TRIS:HEMA 1:1 ratio was analyzed to determine whether it was truly a mix between the TRIS and HEMA monomers. The results obtained did indicate there were still alcohol groups present with a broad peak at 3443 cm^{-1} and the strong silicon-oxygen bond peak at 1049 cm^{-1} (Figure 5). The presence of these two peaks confirmed the success of our co-polymerization of TRIS and HEMA. As with all of the other FTIR results peaks were present at roughly 3000 cm^{-1} and 1723 cm^{-1} confirming the presence of carbon-hydrogen bonds and the ester bonds, respectively (Figure 5).

Cell Viability Quantification:

Preliminary results on cell attachment to the polymers was done in collaboration with Dr. Heather Chandler in the College of Optometry at The Ohio State University. Primary canine fibroblasts were seeded onto all polymers. The HEMA polymer sample killed the cells most likely due to dissolution of low molecular weight components. There was clear cell attachment across all polymers (Figure 6). These results qualitatively showed fairly similar amounts of cells

among all of the polymers except for the pure HEMA and TRIS:HEMA 1:3 polymer. Quantitative results were not obtained in this experiment but were obtained later in separate cell experiments.

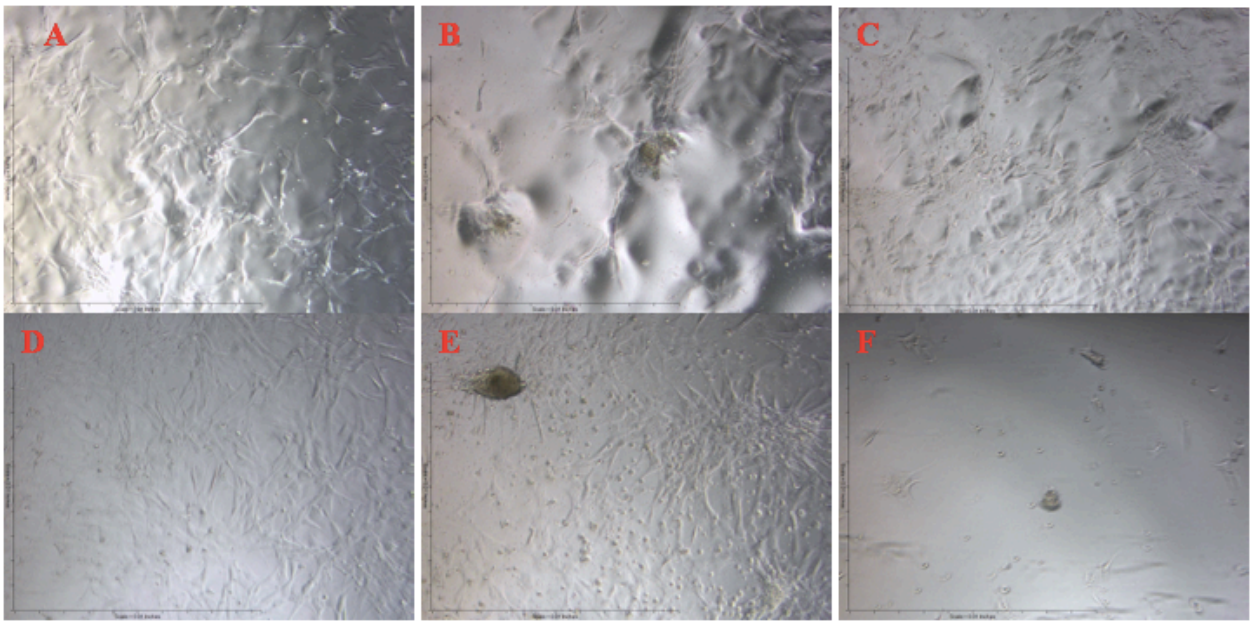

Figure 6: Light microscopy images of K9 fibroblasts on polymers (excluding HEMA). (A) TRIS, (B) T:H 3:1, (C) T:H 2:1, (D) T:H 1:1, (E) T:H 1:2, (F) T:H 1:3.

Following these preliminary results mouse NIH 3T3 cells were seeded onto all seven polymers and a control well without any coating (polystyrene). At five days, it could be seen that the cells preferred polymers with higher content of TRIS than HEMA. It can be seen that the TRIS polymer in Figure 7A had more cells attached than the following polymers.

It should be noted that for both the T:H 1:3 and HEMA polymers the films did not completely coat the bottom of the well plate probably due to the higher viscosity and hydrophilicity of these two polymer solutions. Because these polymer films did not coat the entire surface of the well there were distinct lines that could be seen where the polymer ended and the polystyrene was exposed. This line is clearly seen in the image below of the T:H 1:3 polymer (Figure 7F). The upper portion of the image where there are many cells attached is where the polystyrene was exposed and the bottom portion of the image shows the polymer

where very few cells were present and attached. Similar to the T:H 1:3 polymer there were clear distinctions between the polymer and polystyrene bottom of the well for the HEMA polymer. Figure 7G1 specifically shows this line, the right side of the image shows the cells attaching to the polystyrene and Figure 7G2 shows very few cells attaching to the HEMA polymer compared to the control. Polystyrene's water contact angle has been measured to be around 90 degrees, making it a more hydrophobic surface (Wang & Porter, 1983). It is possible that when the polymer films formed the side groups for HEMA, due to their increased flexibility, were turned in. This would make the surface smoother and limit cell attachment. This could also explain why cells proliferated the most on the polystyrene surface as compared to the polymer films. In the future, preferential attachment studies can be designed to evaluate whether the cells will migrate onto the polymer surface.

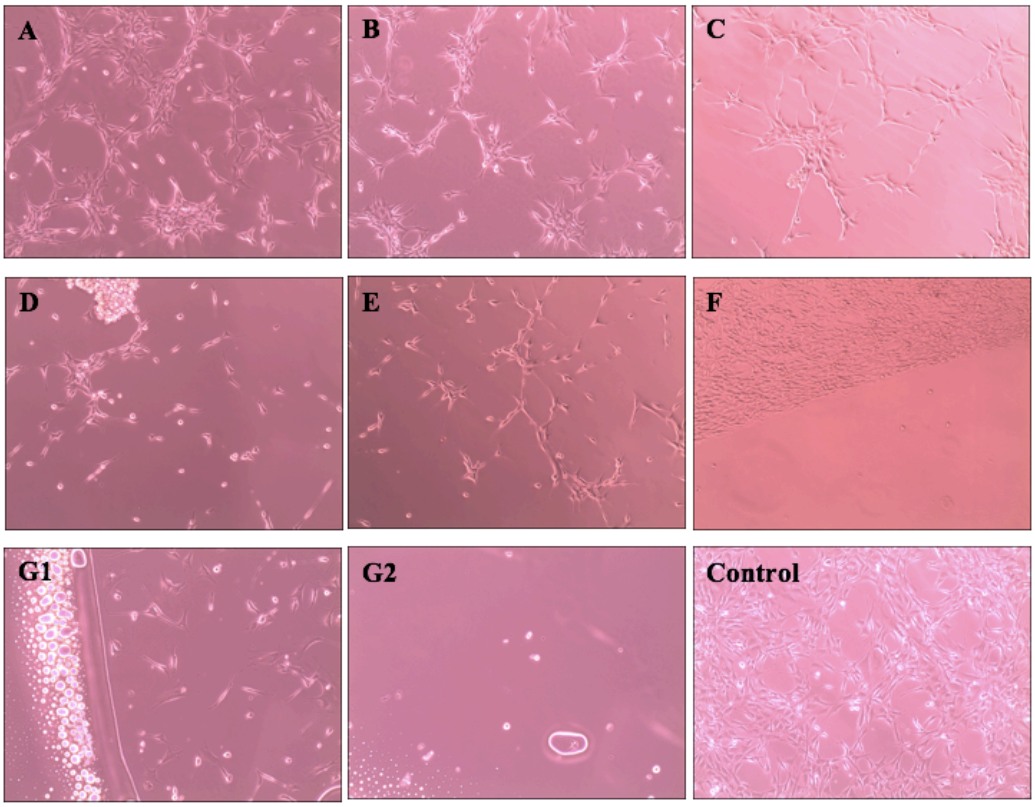

Figure 7: Light microscopy images of NIH 3T3 cells on polymers and control at day 5. (A) TRIS, (B) T:H 3:1, (C) T:H 2:1, (D) T:H 1:1, (E) T:H 1:2, (F) T:H 1:3, (G1&G2) HEMA, Control (polystyrene)

The images from these experiments imply that the fibroblast cells preferred polymers with more TRIS present. Following qualitative analysis, an MTS assay was performed and the results were plotted. The results confirm the qualitative analysis that the fibroblast cells preferred polymer surfaces with TRIS present and the pure TRIS polymer produced the best cell viability (Figure 8) (Table 3). However, the mixed ratio polymers produced varying results suggesting that the film surface presented may not be representative of the polymer composition. Altered surface chemistry or topography may have prevented cell attachment.

This study looked into determining which polymers synthesized produced the best cell viability and attachment. However, since fibroblasts were used instead of corneal epithelial cells TRIS may not be the best option moving forward. As previously stated, over proliferation of fibroblasts causes corneal haze and scarring. Therefore, a surface that allows maximum fibroblast attachment and proliferation is not preferable and based on the data one of the amphiphilic polymers would be preferable.

Table 3: Data acquired from MTS assay including standard deviation of average absorbances

	Viability %	Average Absorbance (nm)	Standard deviation
TRIS	92.53	3.42	0.23
TH 3:1	51.71	1.91	0.30
TH 2:1	47.75	1.77	0.43
TH 1:1	51.68	1.91	0.12
TH 1:2	66.63	2.46	0.08
TH 1:3	51.55	1.91	0.03
HEMA	21.42	0.79	0.02

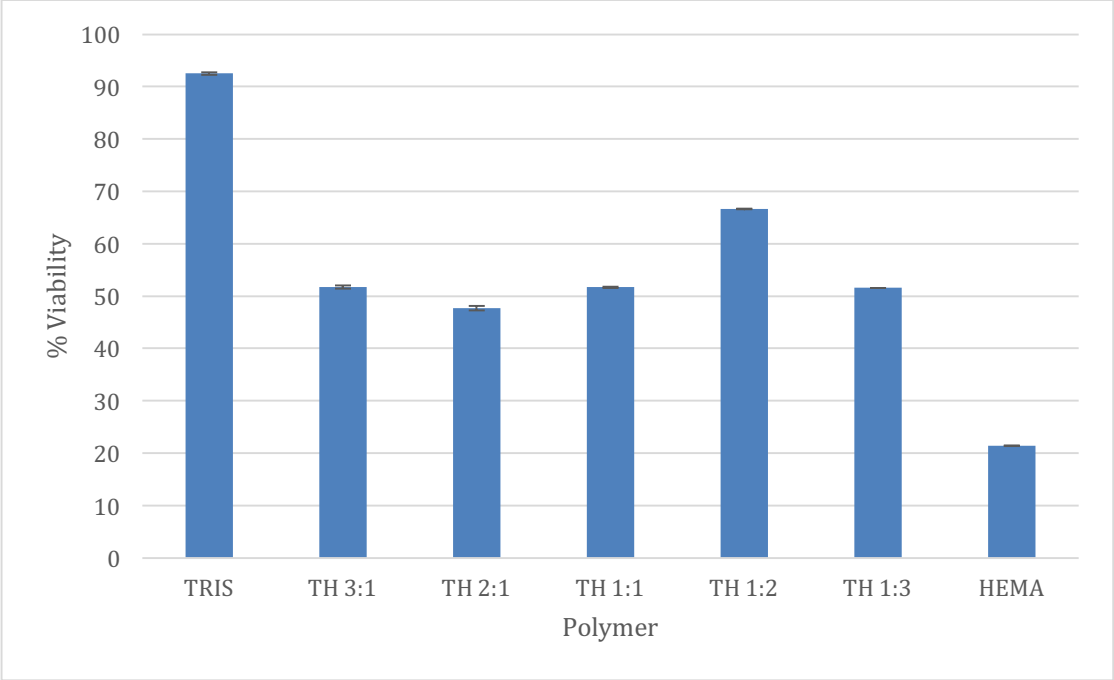

Figure 8: Graph of cell viability

Conclusion:

Contact angle and surface free energy testing was inconclusive in characterizing the polymers. The FTIR results were able to prove successful co-polymerization of the TRIS and HEMA polymers along with casting doubt on the possibility that the unusual contact angle and surface free energy results were due to the polymer rotating alcohol groups. Further work will need to be done to develop improved film casting techniques along with optimizing the contact angle and surface free energy testing by implementing receding and advancing contact angle measurements. Improved film casting techniques may be accomplished by optimizing the solvent to polymer ratio when dissolving the polymers or by using different pipetting techniques when casting the films.

Through this study it was determined that the NIH 3T3 fibroblast cells preferred surfaces with more TRIS; with the pure TRIS polymer exhibiting the highest cell viability. However, more research must be conducted to determine why the HEMA polymer synthesized in this study

produced such unusual contact angle and surface free energy results that implied the polymer was hydrophobic and why there was no clear trend in the obtained goniometer data.

Better film casting techniques along with more contact angle studies will be performed to better characterize the chemistry of the polymers synthesized in future experiments. Mechanical properties will also be characterized utilizing a rheometer. In terms of fibroblast attachment, one of the amphiphilic copolymers would be ideal based on the results of this study. Future studies will specifically look into how corneal epithelial cells attach and proliferate on the polymer films. Once these tests are completed the results from all of the cell studies will be further analyzed to find an optimal polymer that has minimal fibroblast attachment and maximum corneal epithelial cell attachment.

Bibliography:

Ashby, B. D., Garrett, Q., & Wilcox, M. D. (2014). Corneal Injuries and Wound Healing – Review of Processes and Therapies, *1*(4), 1–25.

Chawla, B., & Singh, R. (2017). Recent advances and challenges in the management of retinoblastoma. *Indian J Ophthalmol*, *65*(2), 133–139. https://doi.org/10.4103/ijo.IJO

De Paiva, C. S., Pflugfelder, S. C., & Li, D.-Q. (2006). Cell Size Correlates with Phenotype and Proliferative Capacity in Human Corneal Epithelial Cells. *Stem Cells*, *24*(2), 368–375. https://doi.org/10.1634/stemcells.2005-0148

Dua, H. S., Gomes, J. A., & Singh, A. (1994). Corneal epithelial wound healing. *The British Journal of Ophthalmology*, *78*(5), 401–8. https://doi.org/10.1136/bjo.78.5.401

Dupps, W. J., & Wilson, S. E. (2006). Exp Eye Research. *Exp. Eye Research*, *83*(4), 709–720. https://doi.org/10.1016/j.exer.2006.03.015.Biomechanics

Maycock, N. J. R., & Marshall, J. (2014). Genomics of corneal wound healing: a review of the literature. *Acta Ophthalmologica*, *92*(3), e170-84. https://doi.org/10.1111/aos.12227

Navaratnam, J., Utheim, T., Rajasekhar, V., & Shahdadfar, A. (2015). Substrates for Expansion of Corneal Endothelial Cells towards Bioengineering of Human Corneal Endothelium. *Journal of Functional Biomaterials*, *6*(3), 917–945. https://doi.org/10.3390/jfb6030917

Riau, A. K., Angunawela, R. I., Chaurasia, S. S., Lee, W. S., Tan, D. T., & Mehta, J. S. (2011). Early corneal wound healing and inflammatory responses after refractive lenticule extraction (ReLEX). *Investigative Ophthalmology and Visual Science*, *52*(9), 6213–6221. https://doi.org/10.1167/iovs.11-7439

Wang, L. -H, & Porter, R. S. (1983). The surface orientation of polystyrene measured by liquid contact angle. *Journal of Applied Polymer Science*, *28*(4), 1439–1445.

https://doi.org/10.1002/app.1983.070280417